

# Organic & Biomolecular Chemistry

Accepted Manuscript



This article can be cited before page numbers have been issued, to do this please use: F. Pandolfi, D. Rocco and L. Mattiello, *Org. Biomol. Chem.*, 2019, DOI: 10.1039/C8OB03077D.



This is an Accepted Manuscript, which has been through the Royal Society of Chemistry peer review process and has been accepted for publication.

Accepted Manuscripts are published online shortly after acceptance, before technical editing, formatting and proof reading. Using this free service, authors can make their results available to the community, in citable form, before we publish the edited article. We will replace this Accepted Manuscript with the edited and formatted Advance Article as soon as it is available.

You can find more information about Accepted Manuscripts in the [author guidelines](#).

Please note that technical editing may introduce minor changes to the text and/or graphics, which may alter content. The journal's standard [Terms & Conditions](#) and the ethical guidelines, outlined in our [author and reviewer resource centre](#), still apply. In no event shall the Royal Society of Chemistry be held responsible for any errors or omissions in this Accepted Manuscript or any consequences arising from the use of any information it contains.

## Synthesis and characterization of new D- $\pi$ -A and A- $\pi$ -D- $\pi$ -A type oligothiophene derivatives†

Fabiana Pandolfi, Daniele Rocco and Leonardo Mattiello\*

Received 00th January 20xx,  
Accepted 00th January 20xx

DOI: 10.1039/x0xx00000x

www.rsc.org/

In this work we present a series of newly synthesized conjugated oligothiophene derivatives, with different numbers of central thiophene units, and different donor/acceptor architectures. Electrochemical and spectroscopic data have also been reported. We used thiophene or bithiophene as central Donor core units, 3-octylthiophenes as  $\pi$ -bridge and solubilizing sub-units, and ethyl cyanoacetate or rhodanine moieties as Acceptor end groups, in order to get D- $\pi$ -A and A- $\pi$ -D- $\pi$ -A molecular architectures. The length of synthesized oligothiophenes ranges from three to eight thiophene units, a variety that is sufficient to put in evidence different optical and electrochemical as well as semiconducting characteristics. Oligothiophene compounds can be regarded not only as models for the study of structure-property relationships relatives to polythiophenes, but also they present a large number of applications in the field of Organic Electronics (*i.e.*: as donors in bulk-heterojunction solar cells as well as hole-transporting layer materials in perovskite solar cells, among others).

### Introduction

Oligomeric<sup>1</sup> and polymeric derivatives of thiophene are probably the most studied and used organic semiconductor materials in the vast field of Organic Electronics.<sup>2,3</sup> They find a huge number of applications as materials employed in devices for, e.g.: Organic Light-Emitting Diodes,<sup>4-7</sup> Organic Photovoltaics,<sup>8-12</sup> Sensors (of various types),<sup>13,14</sup> Organic Field-Effect Transistors,<sup>15,16</sup> Organic Photodetectors,<sup>17</sup> and many more. The main advantages possessed by thiophene derivatives over other classes of conjugated compounds are represented, principally, by their excellent charge transport properties and well-established synthetic procedures. Despite the fact that polythiophenes were the first and most used thiophene derivatives, they suffer from several points of view (e.g.: the lack of well-defined chemical structures, the presence of impurities and the presence of defects in molecular structures) whereas a high grade of purity and synthetic reproducibility are requested, in order to clearly address the syntheses of materials with precise and specific properties. In this respect, oligothiophene molecules represent the perfect compromise between purity and performance.<sup>18-20</sup> They can be regarded either as model compounds for the study of structure-property relationships relatives to polythiophenes, and as self-consistent materials that can possess unique and superior characteristics (physico-chemical, optical, electronic, self-assembly properties, possibility to work

in solution, ease of purification, low-cost synthetic procedures, and so on) over their polymeric counterparts.

As an example, in the field of Organic Photovoltaics, dipolar push-pull chromophores with highly polarizable  $\pi$ -electron systems with donor (D) and acceptor (A) groups possess properties that result from the existence of photoinduced intramolecular charge transfers at quite low energies. Among small molecules, thiophene oligomers possess extended  $\pi$ -electron delocalization along the backbone and are good hole-transporting materials.<sup>21,22</sup>

### Results and Discussion

#### Synthesis

We synthesized a number of novel conjugated oligothiophenes with different numbers of central thiophene units, and different donor/acceptor architectures. The “molecular template” we adopted in this work, depicted in Chart 1, is quite self-explanatory and well represents our general synthetic approach.

Two types of “donor core” were chosen in this work: thiophene and 2,2'-bithiophene. The length of the “oligothiophene backbone” depends on the number of 3-alkylated thiophene units and on the kind of central donor core.

Generally speaking, several kind of groups with different conjugation systems and electron-withdrawing capabilities can be used as acceptor end-capping groups. In this work we mainly adopted the ethyl cyanoacetate moiety and, in some cases, also the rhodanine fragment, which is also a dye unit.

In this way, we obtained two types of architectures: D- $\pi$ -A and A- $\pi$ -D- $\pi$ -A, that, along with the possibility to use different backbone lengths and different end-capping groups, can lead

Dept. of Basic and Applied Sciences for Engineering, Sapienza University of Rome  
Via del Castro Laurenziano 7, 00161 Rome, Italy.

†Electronic Supplementary Information (ESI) available: photographs of solutions of compounds; experimental procedures; absorption UV-Vis spectra; <sup>1</sup>H-NMR and <sup>13</sup>C-NMR spectra. See DOI: 10.1039/x0xx00000x

to oligothiophene derivatives possessing different physico-chemical, optical and electrochemical properties such as wavelength range of absorption, bandgap and so on.

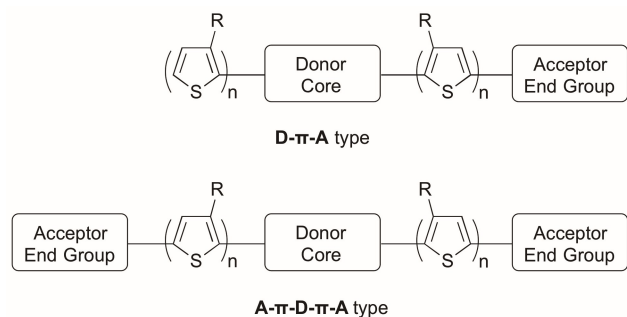


**Chart 1** D- $\pi$ -A and A- $\pi$ -D- $\pi$ -A molecular architectures adopted in this work. Thiophene and 2,2'-bithiophene were used as Donor Core, and ethyl cyanoacetate or 3-ethylrhodanine as precursors of Acceptor End Groups. R = n-octyl; n = 1, 2, 3.

For a better fluency and comprehension of the text, in Chart 2 are reported all synthesized oligothiophenes.

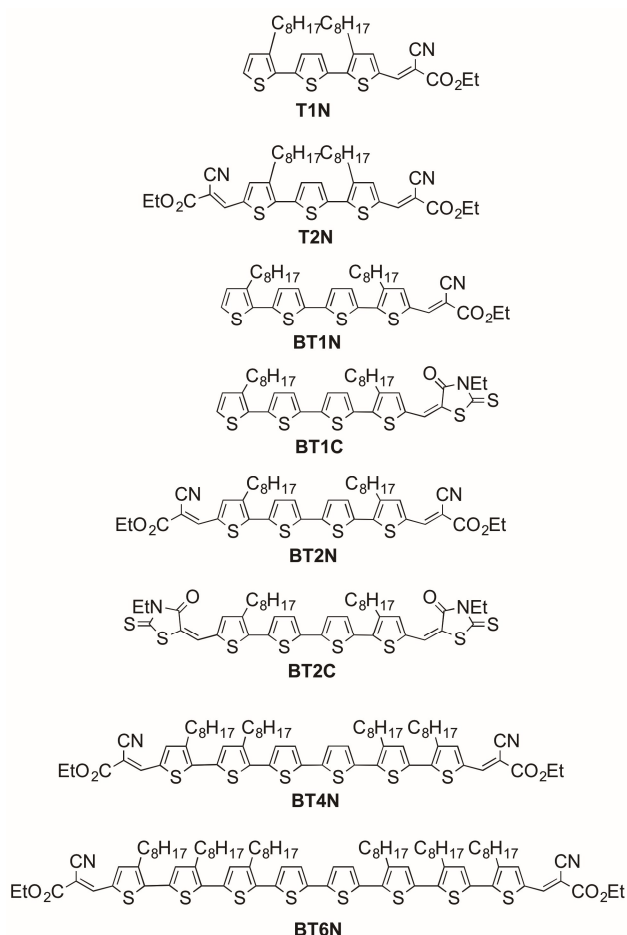
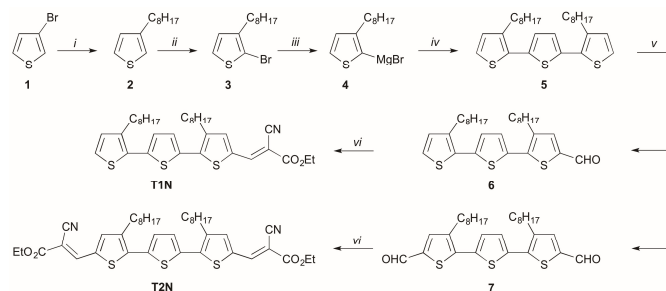


**Chart 2** General scheme of all synthesized oligothiophenes.

The first synthetic route, depicted in Scheme 1, regards the syntheses of **T1N** (ethyl 2-cyano-3-(3,3'-dioctyl-[2,2':5',2''-terthiophene]-5-yl)acrylate) and **T2N** (diethyl 3,3'-[3,3''-dioctyl-[2,2':5',2''-terthiophene]-5,5''-diyl]bis(2-cyanoacrylate)).



**Scheme 1** Synthesis of **T1N** and **T2N**. Reaction conditions: i) octylmagnesium bromide, Et<sub>2</sub>O, Ni(dppp)Cl<sub>2</sub>; ii) N-bromosuccinimide, CHCl<sub>3</sub>-AcOH; iii) Mg, THF, 1,2-dibromoethane; iv) 2,5-dibromothiophene, THF, Ni(dppp)Cl<sub>2</sub>; v) POCl<sub>3</sub>, DMF, 1,2-dichloroethane; vi) triethylamine, ethyl cyanoacetate, DCM.

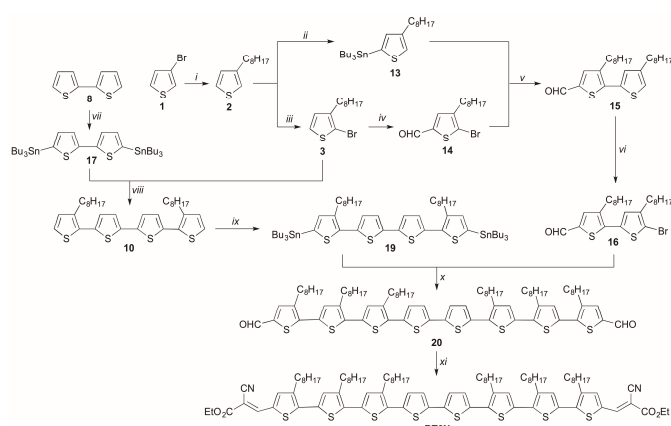
The first step is the synthesis of 3-octylthiophene **2**, obtained in quantitative yield by a Kumada coupling reaction<sup>23</sup> between two commercial products, namely, 3-bromothiophene **1** and octylmagnesium bromide (2 M ether solution), in the presence of a Nickel catalyst as dichloro[1,3-bis(diphenylphosphino)propane] nickel (II) (Ni(dppp)Cl<sub>2</sub>) which was readily synthesized in excellent yields in an open vessel from nickel(II) chloride hexahydrate and 1,3-bis(diphenylphosphino)propane.<sup>10</sup> The Nickel catalyst can be stored in anhydrous conditions and remains active for several months. The second step is the bromination of 3-octylthiophene **2** with *N*-bromosuccinimide (NBS) at 0 °C using a chloroform-acetic acid mixture (1:1 v/v) as solvent.<sup>24,25</sup> The brominated product, 2-bromo-3-octylthiophene **3** was obtained in quantitative yield. Then, starting from **3**, the Grignard reagent **4** (2-(3-Octylthienyl)magnesium bromide) was obtained and used immediately in the subsequent Kumada coupling reaction with 2,5-dibromothiophene to give 4,4''-dioctyl-2,2':5',2''-terthiophene **5** with a 69% yield.<sup>26</sup> The following step was the Vilsmeier-Haack formylation<sup>27</sup> with phosphorus oxychloride and *N,N*-dimethylformamide (DMF) that allowed us to obtain in a single reaction step, with a ratio of 2:1 respectively, the mono- and the di-formylated adducts: 3,3''-dioctyl-[2,2':5',2''-terthiophene]-5-carbaldehyde **6** and 3,3''-dioctyl-[2,2':5',2''-terthiophene]-5,5''-dicarbaldehyde **7**, with an overall very good yield, respectively, 58% (**6**) and 31% (**7**). The final step, a Knoevenagel condensation<sup>28</sup> between ethyl cyanoacetate and compounds **6** and **7**, allowed us to obtain the target compounds, respectively, **T1N** (63% yield) and **T2N** (64% yield). Between all the synthesized oligothiophenes, only **T2N** presents a bibliographic reference<sup>29</sup> (a patent), nevertheless it was also included in our synthetic plan for comparison purposes.

The synthetic route depicted in Scheme 2 regards the syntheses of **BT1N**, (ethyl 2-cyano-3-(3,3''-dioctyl-[2,2':5',2''-5',2''-quaterthiophen]-5-yl)acrylate), **BT1C** (5-((3,3''-dioctyl-[2,2':5',2''-5',2''-quaterthiophen]-5-yl)methyl-end)-3-ethyl-2-thioxothiazolidin-4-one), **BT2N** (diethyl 3,3'-[3,3''-dioctyl-[2,2':5',2''-5',2''-quaterthiophen]-5,5''-diyl]bis





Knoevenagel condensation to give the last target compound BT6N, as a black solid, with a 74% yield.



**Scheme 4** Synthesis of **BT6N**. Reaction conditions: i) octylmagnesium bromide, Et<sub>2</sub>O, Ni(dppp)Cl<sub>2</sub>; ii) n-BuLi, THF, (Bu)<sub>3</sub>SnCl; iii) *N*-bromosuccinimide, CHCl<sub>3</sub>-AcOH; iv) POCl<sub>3</sub>, DMF, 1,2-dichloroethane; v) Pd(PPh<sub>3</sub>)<sub>4</sub>, toluene; vi) *N*-bromosuccinimide, CHCl<sub>3</sub>-AcOH; vii) n-BuLi, THF, (Bu)<sub>3</sub>SnCl; viii) Pd(PPh<sub>3</sub>)<sub>4</sub>, toluene; ix) n-BuLi, THF, (Bu)<sub>3</sub>SnCl; x) Pd(PPh<sub>3</sub>)<sub>4</sub>, toluene; xi) triethylamine, ethyl cyanoacetate, DCM.

### Optical Absorption Properties

The optical absorption spectra of target compounds **T1N**, **T2N**, **BT1N**, **BT2N**, **BT1C**, **BT2C**, **BT4N**, **BT6N** (and compounds **5** and **10**, for comparison) in dichloromethane solution were measured by UV-Vis spectroscopy. Optical band gaps were determined from  $\lambda_{\text{onset}}$ .<sup>35</sup> All the UV-Vis spectra are shown in Electronic Supplementary Information (ESI) and the corresponding data are listed in Table 1. All molecules reveal an intense band attributed to the  $\pi$ - $\pi^*$  transition of the conjugated oligothiophene system.<sup>33</sup> Compound **5**, having as donor core only one thiophene unit, displays a maximum absorption peak ( $\lambda_{\text{max}}$ ) at 338 nm. Changing the central core with 2,2'-bithiophene group, as in compound **10**, causes a red-shift of the maximum absorption peak ( $\lambda_{\text{max}}$ ) to 379 nm. If an electron withdrawing group is introduced, as an acceptor end unit, it is observed a red-shift of  $\lambda_{\text{max}}$ , depending on the type and number of electron withdrawing groups (Figure 1). In fact, the maximum wavelength is observed for oligothiophene **BT2C** ( $\lambda_{\text{max}} = 508$  nm), that contains two rhodanine moieties as acceptor end groups.

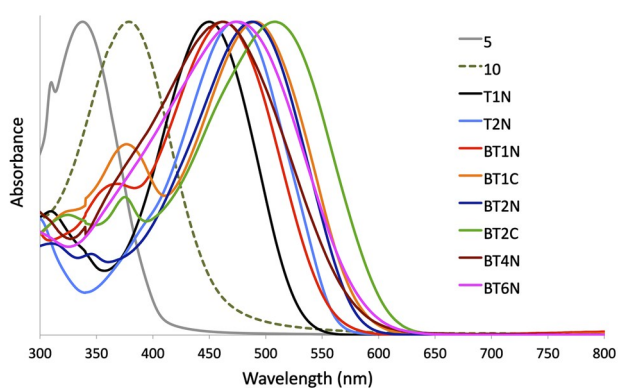


**Figure 1** Normalised optical absorption spectra in DCM solution.

Each of the Figures of the absorption spectra present in the ESI shows a comparison between two compounds. By observing the series of Fig. 3S (**T1N** and **T2N**), Fig. 4S (**BT1N** and **BT2N**) and Fig. 7S (**BT1C** and **BT2C**) it is clear the red-shift caused by the change of the molecular architecture from the D- $\pi$ -A type to the A- $\pi$ -D- $\pi$ -A type, all other things like donor core and acceptor end units being equal, for each couple. Fig. 5S (**T1N** and **BT1N**) and Fig. 6S (**T2N** and **BT2N**) show clearly the same effect but caused by the change of donor core, being equal, this time, the type of molecular architecture and the type acceptor end units. Finally, Fig. 8S (**BT1N** and **BT1C**) and Fig. 9S (**BT2N** and **BT2C**), reveal also that the same effect in red-shifting the absorbance peaks was caused by the change of the acceptor end units from an ethyl cyanoacrylate moiety to a more powerful electron withdrawing group unit such as rhodanine; in this case being equal, this time, the type of molecular architecture and the donor core. Only **BT4N** and **BT6N** compounds (Fig. 10S) show an unexpected optical behaviour regarding the value of  $\lambda_{\text{max}}$ , being the only two molecules that do not respect *entirely* the red-shift trends observed for the rest of the series. At this time we do not have formulated any clear hypothesis about this behaviour. In fact, comparing **BT2N** ( $\lambda_{\text{max}} = 489$  nm) with **BT4N** ( $\lambda_{\text{max}} = 462$  nm) and **BT6N** ( $\lambda_{\text{max}} = 475$  nm), it is observed a linear red-shift between **BT4N** and **BT6N**, but not with respect to **BT2N**. However,  $\lambda_{\text{onset}}$  data in the series **T2N**, **BT2N**, **BT4N** and **BT6N** *completely* follow the expected red-shift trend.

**Table 1.** Absorption data of compounds in DCM solution. C=2x10<sup>-5</sup> M.  $E_g^{\text{opt}}$  calculated from  $\lambda_{\text{onset}}$ .

compound	$\lambda_{\text{max}}$ (nm)	$\lambda_{\text{onset}}$ (nm)	$E_g^{\text{opt}}$ (eV)
<b>5</b>	338	401	3.09
<b>10</b>	379	456	2.72
<b>T1N</b>	451	528	2.35
<b>T2N</b>	473	560	2.21
<b>BT1C</b>	491	581	2.13
<b>BT1N</b>	462	553	2.24
<b>BT2C</b>	508	604	2.05
<b>BT2N</b>	489	576	2.15
<b>BT4N</b>	462	578	2.15
<b>BT6N</b>	475	584	2.12

The  $\lambda_{\text{onset}}$  values for all compounds show the same trend of  $\lambda_{\text{max}}$ , increasing with number of thiophene units and withdrawing acceptor end group. Indeed, in the series containing ethyl cyanoacrylate moiety as electron withdrawing group, **BT6N** shows the highest value of  $\lambda_{\text{onset}}$ , as reported in Table 1. Since the optical band gap ( $E_g^{\text{opt}}$ ) of these compounds is calculated from the  $\lambda_{\text{onset}}$ , its value decreases with the change of the molecular architecture from the D- $\pi$ -A type to the A- $\pi$ -D- $\pi$ -A type and with the change of withdrawing acceptor end group. In fact, **BT2C**, which contains rhodanine fragment, shows the lowest value. This behaviour can be attributed to the great stabilization of the LUMO level by the electron-withdrawing groups.<sup>37</sup> These compounds show trends in their optical properties that are in line with their different conjugation lengths, molecular architectures and acceptor end units. This optical behaviour left room for further studies directed to the improvement of internal conjugation by the modification of

the architecture of these new oligothiophenes, *e.g.*, by simply changing the nature of accepting end groups.

### Optical Emission Properties

The optical emission spectra of target compounds **T1N**, **T2N**, **BT1N**, **BT2N**, **BT1C**, **BT2C**, **BT4N**, **BT6N**, in dichloromethane solution, were measured by fluorescence spectroscopy. The corresponding data are listed in Table 2 and depicted in Figure 2.

**Table 2.** Fluorescence emission data of compounds in DCM solution.  $C=10^{-5}\pm 10^{-6}$  M.

compound	$\lambda_{\max}$ (nm)
<b>T1N</b>	594
<b>T2N</b>	576
<b>BT1C</b>	-
<b>BT1N</b>	662
<b>BT2C</b>	688
<b>BT2N</b>	621
<b>BT4N</b>	-
<b>BT6N</b>	-

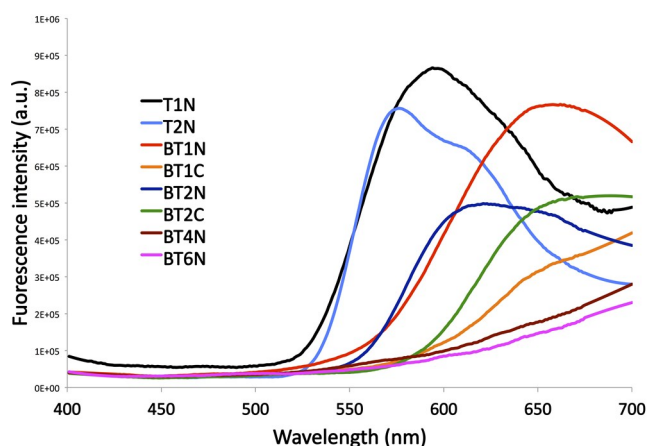


**Figure 2** Fluorescence emission spectra in DCM solution.

In the series of these target compounds, an evident diminution of the intensity of the emission bands with the extension of the conjugated thiophene backbone can be observed.<sup>27</sup> Moreover, also a red-shift is clearly observed as the number of thiophene units increases. For this reason, for three (out of eight) oligomers has not been possible to measure  $\lambda_{\max}$ , because the maximum emission intensity falls in the infrared region. All of these results are in accordance with an expected strong intramolecular charge transfer from the thiophene (or bithiophene) donor core to the cyanoacrylate acceptor end groups.

### Electrochemical Properties

Cyclic voltammetry (CV) was used to investigate the energy levels of target compounds and the related data are presented in Table 3. The potentials were internally calibrated using the

ferrocene/ferrocenium (Fc/Fc<sup>+</sup>) redox couple. The energy levels of the highest occupied molecular orbitals (HOMOs) and lowest unoccupied molecular orbitals (LUMOs) were calculated from the onset oxidation and reduction potentials.<sup>38</sup> The HOMO levels increase from -5.68 to -5.14 eV with increasing conjugation length, as expected, in the series **T2N**, **BT2N**, **BT4N** and **BT6N**, with thiophene units ranging from three to eight, but with the same A- $\pi$ -D- $\pi$ -A architecture and same acceptor end groups. The data from Table 3 also indicate that also the lowering of the electrochemical bandgaps ( $E_g^{\text{elec}}$ ) is highly predictable on the basis on the same three factors observed in the analysis of the optical properties, namely, the donor core, the type of molecular architecture and the acceptor end units.

**Table 3.** Electrochemical data of compounds in 0.1 M TBABF<sub>4</sub>/DCM solution.  $C=1\times 10^{-3}$  M. GC electrode, Pt wire, SCE reference electrode. Sweep rate = 100 mV s<sup>-1</sup>.  $E^\circ(\text{Fc}^+/\text{Fc}) = +0.46$  V vs SCE.

molecule	$E^{\text{ox}}_{\text{onset}}$ (V)	$E^{\text{red}}_{\text{onset}}$ (V)	$E_{\text{HOMO}}$ (eV)	$E_{\text{LUMO}}$ (eV)	$E_g^{\text{elec}}$ (eV)
<b>T1N</b>	1.14	-0.98	-5.54	-3.42	2.12
<b>BT1N</b>	0.96	-1.00	-5.36	-3.40	1.96
<b>BT1C</b>	0.94	-0.92	-5.34	-3.48	1.86
<b>BT2C</b>	0.90	-0.90	-5.30	-3.50	1.80
<b>T2N</b>	1.28	-0.80	-5.68	-3.60	2.08
<b>BT2N</b>	1.07	-0.95	-5.47	-3.45	2.02
<b>BT4N</b>	0.82	-0.96	-5.22	-3.44	1.78
<b>BT6N</b>	0.74	-0.94	-5.14	-3.46	1.68

In order to make a more in-depth analysis we report, in Figure 3, the voltammetric curves obtained for compounds **T1N**, **BT1N**, **T2N** and **BT2N**.

Interpreting the results coming from voltammetric experiments, several interesting observations can be made. **T1N** and **BT1N** oligothiophenes present a free alpha- position at one end of the molecule. This leads to an irreversible oxidation wave that clearly indicates a subsequent chemical reaction, *i.e.*, a dimerization. On the other hand, for **T2N** and **BT2N** no free alpha- positions are available, with the consequence of having reversible oxidation waves for both the oligomers.

**BT2N** presents two reversible oxidation waves as compared with the single reversible oxidation wave possessed by **T2N**. This fact, along with the negative potential shift presented by the first oxidation wave of **BT2N** respect to that one of **T2N**, is in line with the increased conjugation length (from three to four thiophene units).<sup>11,39</sup> The other studied oligothiophenes (whose voltammetric curves are not depicted) follow the same trend from the point of view of the negative potential shift of the oxidation waves.

The irreversible reduction behaviour of **T1N** and **BT1N** molecules indicates a well-known reaction pattern presented by similar structures.<sup>40,41</sup> Moreover, the presence of a second electron-withdrawing group, in **T2N** and **BT2N**, give rise to a reversible (and quasi-reversible) behaviour, probably due to a stabilization of the radical anion along the oligothiophene backbone.

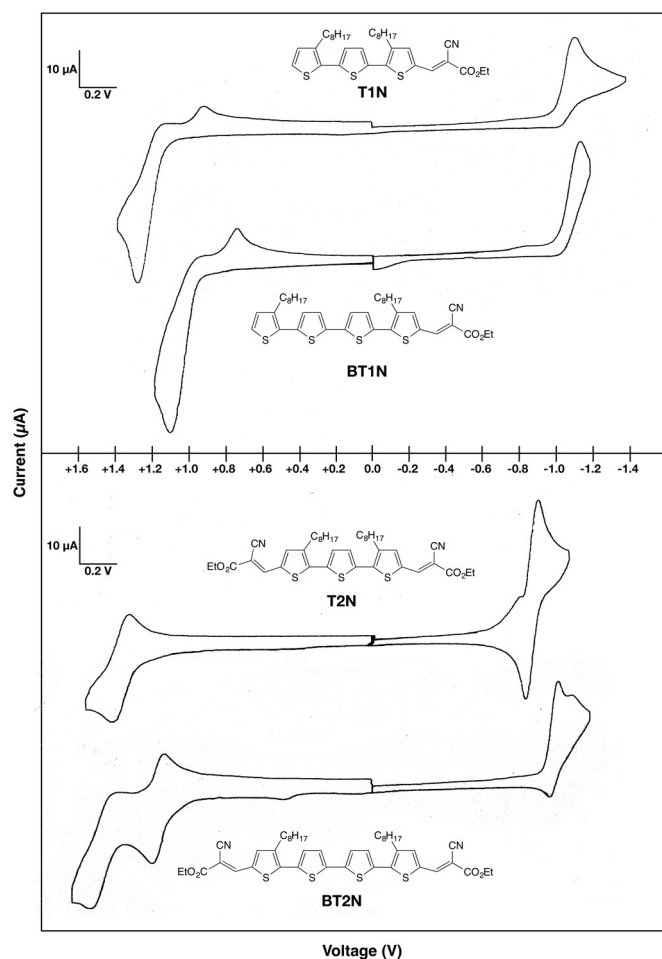


**Figure 3** Voltammetric curves of compounds **T1N**, **BT1N**, **T2N** and **BT2N**. 0.1 M TBABF<sub>4</sub>/DCM solution. C=1x10<sup>-3</sup> M. GC electrode, Pt wire, SCE reference electrode. Sweep rate = 100 mV s<sup>-1</sup>. E°(Fc<sup>+</sup>/Fc) = +0.46 V vs SCE.

The E<sub>g</sub> values obtained from voltammetric experiments conducted on the series of A-π-D-π-A oligothiophenes are in a range from 2.0 eV to 1.7 eV. These values fall in the same range possessed by oligothiophenes with comparable structures that present as of today the best photovoltaic performances in the field of oligothiophenes.<sup>11</sup>

The results obtained for these newly synthesized compounds underline the importance that these kind of oligothiophene derivatives possess in the field of organic semiconductors: inexpensive and reproducible chemical syntheses, ease of purification and good solubility in common organic solvents (necessary requirements for their use in every field of interest for Organic Electronics, and, often, issues for their polymeric counterparts), chemical and thermal stabilities, and well-established optical and electrochemical properties that, moreover, are finely tunable by the means of organic synthesis.

## Conclusions

We synthesized a number of novel conjugated oligothiophenes with different numbers of central donor core thiophene units (one or two), different donor/acceptor architectures (namely, D-π-A and A-

π-D-π-A) and different acceptor end units (from the Knoevenagel condensation with ethyl cyanoacetate and 3-ethylrhodanine).  
DOI: 10.1039/C8OB03077D

The oligomers synthesized in this way possess from three to eight thiophene backbone units and this situation allowed us to get useful information from their electrochemical and optical properties: in fact, these new oligothiophenes possess low bandgaps, a condition required for their applications in several fields of Organic Electronics, and there are also clear evidences that they represent promising candidates for future studies directed to fine-tune their optical, electrochemical and morphological properties in order to satisfy the requirements coming from the different fields of application of organic semiconductors.

## Experimental

Unless otherwise stated, starting materials were used as purchased without further purification. Diethyl ether and tetrahydrofuran (THF) were freshly distilled from sodium-benzophenone before use. Reactions were performed under nitrogen atmosphere with standard laboratory equipment and, when required, by the means of a Schlenk apparatus. The detailed synthetic procedures and characterization data are provided in the Electronic Supplementary Information (ESI). The catalyst dichloro[1,3-bis(diphenylphosphino)propane] nickel (II) (Ni(dppp)Cl<sub>2</sub>) used in the Kumada coupling reactions was synthesized using published procedures.<sup>42</sup> N-bromosuccinimide (NBS) used in the bromination reactions was purified by the means of standard procedures.<sup>24</sup> The removing of tin by-products (if any) present in the mixtures from stannylation reaction and Stille reaction, were performed by the means of potassium fluoride aqueous solution washings.<sup>43</sup> Thin layer chromatography was carried out using Alugram SIL G/UV254 plates and visualized under UV light (at 254 and/or 365 nm). Flash chromatography was carried out using Silica Gel 60 (0.04-0.063 mm). <sup>1</sup>H and <sup>13</sup>C NMR spectra were measured on a Bruker AVANCE 200 MHz spectrometer at 200 and 50 MHz respectively. The residual signals for the NMR solvent (CDCl<sub>3</sub>) are 77.16 ppm (<sup>13</sup>C) and 7.27 (<sup>1</sup>H); the following abbreviations have been used for NMR assignment: s for singlet, d for doublet, t for triplet and m for multiplet. APCI mass spectra were measured on a LC/MS-MS Thermo Scientific TSQ Quantum Access Max spectrometer. The absorption spectra were measured with a Jasco V-750 double beam spectrophotometer in the 300÷800 nm range in a 3 mL cuvette. The samples for UV-Vis spectra were prepared diluting the solution in two mL of DCM to obtain an absorbance included in the range 0.1÷0.2 at 370 nm. The photoluminescence spectra were measured with a Fluoromax 4 plus (Horiba Yobin Yvon) fluorimeter at the excitation wavelength of 370 nm. The emission interval was maintained constant for all the samples in the 400÷700 nm interval. Voltammetric experiments were performed using an AMEL System 5000 apparatus. Measurements were carried out, under nitrogen atmosphere, in a conventional three electrode cell with a saturated calomel electrode with multiple junctions

as the reference electrode,<sup>44</sup> a Pt wire as the counter electrode and a glassy carbon electrode (GCE) as the working electrode. Prior to experiments, the glassy carbon electrode was polished with alumina paste 0.05  $\mu\text{m}$ . All experiments were carried out at 25  $^{\circ}\text{C}$ , in anhydrous dichloromethane (DCM) with 0.1 M tetrabutylammonium tetrafluoroborate (TBABF<sub>4</sub>) as supporting electrolyte at a scan rate of 100  $\text{mV s}^{-1}$ . The concentration of all the substrates was  $1 \times 10^{-3}$  M. In these conditions the standard redox potential of the ferrocenium/ferrocene system is  $E^{\circ}(\text{Fc}^+/\text{Fc}) = +0.46$  V vs SCE. Melting points were determined with a Büchi apparatus and were uncorrected.

## Conflicts of interest

There are no conflicts of interest to declare.

## Acknowledgements

The authors acknowledge Sapienza University of Rome for financial support. The authors are grateful to Dr. Francesco Antolini and Prof. Francesco Michelotti.

## References

- 1 K. Müllen and G. Wegner ed., *Electronic Materials: The Oligomer Approach*, Wiley-VCH, Weinheim, 1998.
- 2 H. Klauk ed., *Organic Electronics: Materials, Manufacturing and Applications*, Wiley-VCH, Weinheim, 2006.
- 3 H. Klauk ed., *Organic Electronics II: More Materials and Applications*, Wiley-VCH, Weinheim, 2012.
- 4 J. Pei, J. L. Wang, X. Y. Cao, X. H. Zhou and W. B. Zhang, *J. Am. Chem. Soc.*, 2003, **125**, 9944–9945.
- 5 X. Li, J. Zhang, G. Huang, Y. Wang, M. Rong, M. Teng and J. Liu, *Dyes and Pigments*, 2017, **141**, 1–4.
- 6 J. S. Cho, Y. Kojima and K. Yamamoto, *Polym. Adv. Technol.*, 2003, **14**, 52–57.
- 7 T. Ozturk, E. Tekin, S. Piravidili Mucur, A. C. Goren, G. Turkoglu, M. E. Cinar and A. Buyruk, US Pat., US20180030069A1, 2018.
- 8 Q. Zhang, B. Kan, F. Liu, G. Long, X. Wan, X. Chen, Y. Zuo, W. Ni, H. Zhang, M. Li, Z. Hu, F. Huang, Y. Cao, Z. Liang, M. Zhang, T. P. Russell and Y. Chen, *Nat. Photonics*, 2015, **9**, 35–41.
- 9 Z. Li, G. He, X. Wan, Y. Liu, J. Zhou, G. Long, Y. Zuo, M. Zhang and Y. Chen, *Adv. Energy Mater.*, 2012, **2**, 74–77.
- 10 Y. Chen, X. Wan and G. Long, *Acc. Chem. Res.*, 2013, **46**, 2645–2655.
- 11 B. Kan, M. Li, Q. Zhang, F. Liu, X. Wan, Y. Wang, W. Ni, G. Long, X. Yang, H. Feng, Y. Zuo, M. Zhang, F. Huang, Y. Cao, T. P. Russell and Y. Chen, *J. Am. Chem. Soc.*, 2015, **137**, 3886–3893.
- 12 (a) K. Lim, M. Kang, Y. Myung, J. Seo, P. Banerjee, T. J. Marks and J. Ko, *J. Mater. Chem. A*, 2016, **4**, 1186–1190; (b) L. Salamandra, L. La Notte, G. Paronesso, G. Susanna, L. Cinà, G. Polino, L. Mattiello, A. Catini, C. Di Natale, E. Martinelli, A. Di Carlo, F. Brunetti, T. M. Brown and A. Reale, *Energy Technol.*, 2017, **131**, 2168–2174.
- 13 T. Sun, Q. Niu, Y. Li, T. Li, T. Hu, E. Wang and H. Liu, *Sens. Actuators, B*, 2018, **258**, 64–71.
- 14 T. Sun, Q. Niu, Y. Li, T. Li, and H. Liu, *Sens. Actuators, B*, 2017, **248**, 24–34.
- 15 R. B. K. Siram, K. Tandy, M. Horecha, P. Formanek, M. Stamm, S. Gevorgyan, F. C. Krebs, A. Kiriy, P. Meredith, P. L. Burn, E. B. Namdas and S. Patil, *J. Phys. Chem. C*, 2011, **115**, 14369–14376. View Article Online  
DOI: 10.1039/C8OB03077D
- 16 C. Zhang and X. Zhu, *Acc. Chem. Res.*, 2017, **50**, 1342–1350.
- 17 O. D. Parashchuk, A. A. Mannanov, V. G. Konstantinov, D. I. Dominskiy, N. M. Surin, O. V. Borshechev, S. A. Ponomarenko, M. S. Pshenichnikov and D. Y. Parashchuk, *Adv. Funct. Mater.*, 2018, **36**, 1800116.
- 18 L. Zhang, N. S. Colella, B. P. Cherniawski, S. C. B. Mannsfeld and A. L. Briseno, *ACS Appl. Mater. Interfaces*, 2014, **6**, 5327–5343.
- 19 G. Turkoglu, M. E. Cinar and T. Ozturk, *Top. Curr. Chem. (Z)*, 2017, **375**:84. doi.org/10.1007/s41061-017-0174-z.
- 20 A. L. Kanibolotsky, N. J. Findlay and P. J. Skabara, *Beilstein J. Org. Chem.*, 2015, **11**, 1749–1766.
- 21 A. Mishra and P. Bäuerle, *Angew. Chem. Int. Ed.*, 2012, **51**, 2020–2067.
- 22 F. Gala, L. Mattiello, F. Brunetti and G. Zollo, *J. Chem. Phys.*, 2016, **144**, 084310.
- 23 X. Guo, R. Ponce Ortiz, Y. Zheng, Y. Hu, Y. Noh, K. Baeg, A. Facchetti and T. J. Marks, *J. Am. Chem. Soc.*, 2011, **133**, 1405–1418.
- 24 H. J. Dauben Jr. and L. L. McCoy, *J. Am. Chem. Soc.*, 1959, **81**, 4863–4873.
- 25 W. Lee, S. K. Son, K. Kim, S. K. Lee, W. S. Shin, S. Moon and I. Kang, *Macromolecules*, 2012, **45**, 1303–1312.
- 26 P. Henderson and D. Collard, *Chem. Mater.*, 1995, **7**, 1879–1889.
- 27 Y. Liu, J. Zhou, X. Wan and Y. Chen, *Tetrahedron*, 2009, **65**, 5209–5215.
- 28 Y. Liu, Y. M. Yang, C. Chen, Q. Chen, L. Dou, Z. Hong, G. Li and Y. Yang, *Adv. Mater. (Weinheim, Ger.)*, 2013, **25**, 4657–4662.
- 29 Y. Chen, X. Wan, Y. Liu, Z. Li, J. Zhou, F. Wang, G. He and G. Long, US Pat., US2014142308A1, 2014.
- 30 N. K. E. Guimard, J. L. Sessler and C. E. Schmidt, *Macromolecules*, 2009, **42**, 502–511.
- 31 B. Kan, M. Li, Q. Zhang, F. Liu, X. Wan, Y. Wang, W. Ni, G. Long, X. Yang, H. Feng, Y. Zuo, M. Zhang, F. Huang, Y. Cao, T. P. Russell and Y. Chen, *J. Am. Chem. Soc.*, 2015, **137**, 3886–3893.
- 32 J. Li, X. Qiao, Y. Xiong, H. Li and D. Zhu, *Chem. Mater.*, 2014, **26**, 5782–5788.
- 33 D. Patra, C. Chiang, W. Chen, K. Wei, M. Wu and C. Chu., *J. Mater. Chem. A*, 2013, **1**, 7767–7774.
- 34 A. Huccke and M. P. Cava, *J. Org. Chem.*, 1998, **63**, 7413–7417.
- 35 J. C. S. Costa, R. J. S. Taveira, C. F. R. A. C. Lima, A. Mendes and L. M. N. B. F. Santos, *Opt. Mater. (Amsterdam, Neth.)*, 2016, **58**, 51–60.
- 36 T. M. Pappenfus, M. W. Burand, D. E. Janzen and K. R. Mann, *Org. Lett.*, 2003, **5**, 1535–1538.
- 37 J. Casado, T. M. Pappenfus, L. L. Miller, K. R. Mann, E. Ortí, P. M. Viruela, R. Pou-Amérigo, V. Hernández and J. T. López Navarrete, *J. Am. Chem. Soc.*, 2003, **125**, 2524–2534.
- 38 H. Zhang, X. Wan, X. Xue, Y. Li, A. Yu and Y. Chen, *Eur. J. Org. Chem.*, 2010, **2010**, 1681–1687.
- 39 B. Nessakh, G. Horowitz, F. Garnier, F. Deloffre, P. Srivastava and A. Yassar, *J. Electroanal. Chem.*, 1995, **399**, 97–103.
- 40 L. Zhou, S. Tu, D. Shi, G. Dai and W. Chen, *Synthesis*, 1998, **1998**, 851–854.
- 41 J. H. P. Utley, M. Güllü and M. Motevalli, *J. Chem. Soc., Perkin Trans. 1*, 1995, **51**, 1961–1970.
- 42 G. R. Van Hecke and W. D. Horrocks, *Inorg. Chem.*, 1966, **5**, 1968–1974.
- 43 E. Le Grogneq, J. M. Chrétien, F. Zammattio and J. P. Quintard, *Chem. Rev.*, 2015, **115**, 10207–10260.
- 44 L. Mattiello and L. Rampazzo, *J. Chem. Soc., Perkin Trans. 2*, 1993, **110**, 2243–2247.